Article

Emotional Contagion Dynamics with Dual Recovery Channels on a Real-World Social Network: An Agent-Based Complex Systems Model

Heng Zhu , Youhu Wang , Mi Zhou *

Posted Date: 23 September 2026

Keywords: emotional contagion; agent-based modeling; complex networks; socio-technical systems; system governance; contagion dynamics; dynamical systems; emotion regulation; social network analysis

 doi:10.20944/preprints202609.1987.v1

Article

Emotional Contagion Dynamics with Dual Recovery Channels on a Real-World Social Network: An Agent-Based Complex Systems Model

Heng Zhu, Youhu Wang and Mi Zhou *

Basic Education College, National University of Defense Technology, Changsha 410073, Hunan, China

* Correspondence: 1838680183@qq.com

Highlights

Contribution to systems science.

- Individual emotional-transition rules are linked to emergent, group-level affective dynamics through an agent-based micro-to-macro analysis.
- A two-channel recovery model (natural recovery vs. capacity-building awareness) provides a mechanism-level, testable basis for controlling collective emotion.

Main findings and implications.

- On a real Facebook network the model generates the characteristic rise–peak–plateau dynamics of collective emotion (peak ≈ 33%, plateau ≈ 28%, $R_0 \approx 1.94$) under baseline parameters, with the aware density systematically lagging the emotion.
- Separating the two recovery channels identifies two distinct intervention levers (environment- vs. capacity-oriented) and predicts that proactive regulation, applied before the peak, narrows the emotion–regulation lag that reactive measures cannot.
- The two channels interact non-trivially: the steady-state fraction that acquires regulation capacity is non-monotonic in both the influence rate and the capacity-building rate, peaking at an interior optimum—so the most resilient population arises from an optimal, not maximal, level of intervention.

Abstract

Collective emotion is an emergent property of social systems: individual affective states propagate along social ties and, in the aggregate, produce group-level patterns that rise, peak, and stabilize. This paper models emotional contagion as a dynamical process on a real social network, extending the susceptible–influenced–susceptible (SIS) framework with a third, aware state—the susceptible–influenced–aware (SIA) model—and separating two recovery routes that earlier single-channel models conflate: natural recovery, the passive fading of an emotional state, and aware recovery, the active acquisition of emotion-regulation capacity that confers partial protection against re-influence. We implement the agent-based model on the Facebook friendship network (N = 4039, E = 88,234). As a theory-building model rather than a data-calibrated one, it generates, under baseline parameters and across 30 independent simulations, a transient peak of roughly 33% influenced density followed by a stable plateau near 28%, with the aware density lagging behind throughout; these are model outcomes, not empirical estimates of real-world prevalence. Mean-field analysis yields a basic reproduction ratio $R_0 = \beta/(\mu + \alpha) \approx 1.94$ governing a transcritical bifurcation between extinction and self-sustaining collective emotion; because the aware channel enters this ratio symmetrically with natural recovery, building regulation capacity is a first-order control on whether collective emotion self-sustains, not merely an aid to recovery. A second analytical result is that the two channels interact non-trivially: the steady-state fraction that acquires regulation capacity is non-monotonic in both the influence rate and the capacity-building rate, peaking at an interior optimum, so the most resilient population is produced by an optimal rather than maximal level of intervention. A social network analysis shows the network is small-world, heavy-tailed, and organized into sixteen strongly

 doi:10.20944/preprints202609.1987.v1

modular communities, with a small set of hub-and-bridge nodes mediating cross-community spread. By representing the two recovery channels as independent parameters, the model separates environment-oriented from capacity-oriented interventions and generates testable predictions for the regulation of collective emotion in digital and organizational settings.

Keywords: emotional contagion; agent-based modeling; complex networks; socio-technical systems; system governance; contagion dynamics; dynamical systems; emotion regulation; social network analysis

1. Introduction

Collective emotion is among the clearest examples of emergence in social systems. Individual affective states—distress, anxiety, enthusiasm—are transmitted through everyday social interaction, and these local exchanges aggregate into group-level patterns that no single member intends: a team becomes anxious under deadline pressure, a community mobilizes around a shared grievance, an online crowd cycles between outrage and calm. Understanding when such collective emotional states arise, how long they persist, and how they subside is a central question for the study of complex social systems.

A robust empirical literature establishes the underlying mechanism. Hatfield and colleagues [1] proposed emotional contagion theory, showing that people unconsciously mimic the expressions, vocalizations, and postures of others and thereby converge emotionally with them; Barsade [2] demonstrated the ripple effect through which one member's emotion shapes group-level affect. Longitudinal and experimental evidence confirms that emotion propagates through real social networks: Fowler and Christakis [3] found that happiness spreads to friends, spouses, and neighbors up to three degrees of separation in the Framingham data, and Kramer and colleagues [4] showed experimentally that emotional states can be transmitted at massive scale through online networks.

These findings motivate a computational treatment. Because emotional states spread through contact and recovery, they have been productively modeled with the mathematics of epidemic spreading [5], which describes how a state propagates across a contact network and either dies out or becomes self-sustaining depending on whether its reproduction ratio exceeds unity. On degree-heterogeneous networks the epidemic threshold can be lowered or even vanish [6,7], so that weakly transmissible states persist through highly connected hubs. Hill and colleagues [8] applied this machinery directly to emotion, introducing the susceptible–infected–susceptible (SIS) model augmented with a spontaneous infection rate—their SISa model—on a large social network. A parallel line of behavioral epidemiology has shown that awareness itself shapes spread: when individuals become aware of a circulating state they reduce their exposure or susceptibility [9], and this awareness–epidemic coupling shifts both the threshold and the equilibrium [10].

Two gaps remain. First, existing contagion models—including SIS, SIR, and the awareness-coupled frameworks—treat recovery as a single, undifferentiated process. Yet the emotion-regulation literature distinguishes two routes by which an emotional state subsides [11]: passive fading, and the active acquisition of regulation capacity through strategies such as cognitive reappraisal and mindfulness [12], which build enduring psychological resources [13]. A single-channel model cannot represent this distinction, and therefore cannot ask which route should be targeted by intervention. Second, most simulation studies report model outcomes without characterizing the topology on which the model runs, leaving it unclear which structural features—degree heterogeneity, clustering, community boundaries—drive the observed dynamics.

The present paper addresses both gaps with a three-state, two-channel model. Building on the SIS framework of Hill et al. [8], we separate natural recovery from aware recovery into two independent channels: influenced individuals either recover passively into susceptibility, or recover into an aware state that confers partial protection against re-influence and itself decays. The protective aware state is thus related to the awareness–epidemic models in which awareness lowers

 doi:10.20944/preprints202609.1987.v1

exposure or susceptibility [9,10], but it differs in emphasis: there, awareness is an information state that weakens transmission, whereas here it is a recovery destination—emotion-regulation capacity acquired in the course of recovering—so that the model splits recovery itself into two parallel channels with independent parameters. Where the SISa model adds a spontaneous infection rate to a two-state SIS process [8], we add a third, aware state and split recovery into natural and capacity-building channels. We implement the model on a real social network—the Facebook friendship network [14,15]—and provide a full social network analysis so that the dynamics can be traced to measurable structural features. We ask whether the model reproduces the characteristic rise–peak–plateau dynamics of collective emotion and whether the dual-recovery structure yields predictions that single-channel models cannot.

The contribution is a systems-level one. Rather than predicting specific episodes, the model sharpens a verbal account of group emotion into executable rules whose emergent consequences—thresholds, equilibria, and time lags—can be inspected directly, following the agent-based tradition in computational sociology and social psychology [16,17]. By keeping the aware state explicit, the model separates two intervention targets—changing environmental conditions versus building regulation capacity—and thereby connects the analysis of contagion dynamics to the practical problem of regulating collective emotion, and situates the work within the systems-science study of socio-technical systems and their governance.

2. Materials and Methods

2.1. The SIA Model: Three States and Five Parameters

We conceptualize group emotional influence as a process in which a specific emotional state—for concreteness, a negative state such as distress or anxiety—spreads among the members of a group. Each individual occupies one of three states. Susceptible individuals are not currently experiencing the target emotion but are open to influence from those who are. Influenced individuals are currently experiencing and expressing the emotion and, by virtue of expressing it, become sources of influence for those around them. Aware individuals have not merely recovered from the emotion but have, in the course of recovering, acquired emotion-regulation capacity—a metacognitive awareness of their own affective states that makes them more resistant to future influence. Because the influenced state is defined by expression, and it is expression that transmits the emotion, the model also treats emotional expression as a social signal that carries information to observers [18].

This distinction is grounded in the emotion-regulation literature. Natural recovery is the passive, homeostatic fading of an emotional state; aware recovery is the active acquisition of regulation ability described by Gross [11], Kabat-Zinn [12], and Fredrickson [13]—recovery that leaves the person better able to manage the emotion should it recur. Crucially, awareness confers a probabilistic rather than absolute buffer: aware individuals are re-influenced at the reduced rate $\beta(1 - p)$, where p $(0 \le p \le 1)$ is the protection factor, and as this capacity fades at rate δ they return to full susceptibility. Awareness is thus a form of partial inoculation that must be maintained. Table 1 summarizes the five parameters and their interpretation.

Two points of interpretation should be made explicit. First, "influenced" denotes an individual who is both experiencing and expressing the target emotion; it is the expressive component—not the private affective state—that constitutes the contagion channel, consistent with the view of emotional expression as a social signal [18]. Second, the aware state is a deliberately stylized proxy for emotion-regulation capacity rather than a strict operationalization of any single psychological construct (such as dispositional mindfulness or reappraisal skill): it condenses the heterogeneous, multi-faceted acquisition of regulation ability into a single rate α. This abstraction trades psychological detail for dynamical tractability while preserving the mechanism—recovery that confers partial, decaying protection—that the model is designed to interrogate.

 doi:10.20944/preprints202609.1987.v1

Table 1. Parameters of the model and their interpretation.

Parameter	Symbol	Interpretation
Influence rate	β	Rate at which an influenced individual converts susceptible neighbors
Natural recovery rate	μ	Passive fading of the emotional state
Awareness formation rate	α	Acquisition of emotion-regulation capacity [11]
Awareness decay rate	δ	Fading of regulation capacity over time
Protection factor	p	Reduction in re-influence susceptibility while aware

The model is deliberately agent-based rather than purely analytical: individuals differ in their network positions—in how many neighbors they have and where they sit relative to dense communities—and these differences, which homogeneous-mixing approximations wash out, are exactly the channels through which group structure shapes influence. An analytical mean-field treatment cannot represent the fact that a highly connected individual is both more exposed to influence and more influential once affected, nor the fact that emotion is funneled along the dense within-community ties that characterize real social groups.

2.2. Model Dynamics and Mean-Field Analysis

The dynamics of the model are defined by five transitions among the three states:

$S + I \rightarrow I + I$ (influence, rate β)

$I \rightarrow S$ (natural recovery, rate μ)

$I \rightarrow A$ (aware recovery, rate α)

$A \rightarrow S$ (awareness decay, rate δ)

$A + I \rightarrow I + I$ (re-influence, rate $\beta(1 - p)$)

At the population level, the mean densities of the three states evolve as

$$dS/dt = -\beta \cdot S \cdot I + \mu \cdot I + \delta \cdot A \quad (1)$$

$$dI/dt = \beta \cdot S \cdot I + \beta(1 - p) \cdot A \cdot I - (\mu + \alpha) \cdot I \quad (2)$$

$$dA/dt = \alpha \cdot I - \delta \cdot A - \beta(1 - p) \cdot A \cdot I \quad (3)$$

The basic reproduction ratio

$$R_0 = \beta / (\mu + \alpha) \quad (4)$$

is the expected number of new influenced individuals generated by a single influenced individual in a fully susceptible population. With the default parameters ($\beta = 0.35$, $\mu = 0.10$, $\alpha = 0.08$, $\delta = 0.02$, $p = 0.5$), $R_0 \approx 1.94$, indicating that emotional influence is, in the aggregate, self-sustaining.

The mean-field system admits two equilibria governed by R_0. The influence-free equilibrium ($S = 1$, $I = 0$, $A = 0$) always exists; linearizing the influenced compartment around it gives $dI/dt \approx (\mu + \alpha)(R_0 - 1) \cdot I$, so it is locally asymptotically stable when $R_0 < 1$ and unstable when $R_0 > 1$. Emotional influence therefore dies out when transmission is outweighed by the combined recovery rates. When $R_0 > 1$, the system admits a unique endemic equilibrium, obtained by setting the three derivatives to zero and using the conservation relation $S + I + A = 1$:

$$S^* = 1 / R_0 - (1 - p) \cdot A^* \quad (5)$$

$$I^* = (R_0 - 1) / R_0 - p \cdot A^* \quad (6)$$

$$A^* = \alpha \cdot I^* / [\delta + \beta(1 - p) \cdot I^*] \quad (7)$$

 doi:10.20944/preprints202609.1987.v1

Substituting Eq. (7) into Eq. (6) yields a quadratic in I*:

$$\beta(1-p)\cdot(I^*)^2 + [\delta + p\alpha - \beta(1-p)(R_0-1)/R_0]\cdot I^* - \delta(R_0-1)/R_0 = 0 \quad (8)$$

whose constant term is negative for $R_0 > 1$, so it has exactly one positive root—the endemic prevalence. The exchange of stability at $R_0 = 1$ is a transcritical bifurcation, the mathematical signature of the phase transition between extinction and self-sustaining collective emotion. The prevalence I* increases with β and δ and decreases with μ, α, and p; the two recovery channels lower it through different routes—μ by draining the influenced state back into susceptibility, α by routing recovery into the buffered aware state.

The aware density A* behaves differently and more interestingly: it is non-monotonic in both β and α, attaining an interior maximum. Two limit arguments establish this. As $\alpha \to 0$ the aware channel vanishes, so $A^* \to 0$; as $\alpha \to \infty$ the reproduction ratio $R_0 = \beta/(\mu + \alpha)$ falls below unity, the influenced state is driven extinct, and the source of awareness dries up, so $A^* \to 0$ again. Likewise $A^* \to 0$ as $\beta \to \mu + \alpha$ from above ($R_0 \to 1^+$) and as $\beta \to \infty$, where the re-influence term $\beta(1-p)\cdot A\cdot I$ drains awareness faster than it is replenished. Because A* is continuous and positive in between, it must attain an interior maximum in each parameter. Intuitively, awareness is fed by the influenced population—its source—and drained by decay and re-influence; too little contagion leaves too few influenced individuals to convert, while too much overwhelms the buffer. The decay rate δ is essential to this optimum: without it ($\delta = 0$) the aware fraction settles at the fixed level $\alpha/[\beta(1-p)]$ regardless of the affected population. The interior optimum is therefore a direct, emergent consequence of the dual-channel structure with finite awareness decay.

2.3. Network Data

We implemented the model on a publicly available real network: the Facebook friendship network compiled by McAuley and Leskovec [14] from the Stanford Network Analysis Project (SNAP) [15]. It comprises 4039 individuals connected by 88,234 undirected friendship ties. Because it is a real rather than synthetic topology, the results speak directly to how emotional influence behaves in the social settings where group influence actually occurs. To establish that the results are not an artifact of a single topology, we also ran the model on a synthetic LFR benchmark with planted community structure (N = 500, E = 3769) [19] and on the email-Eu-core communication network (N = 1005, E = 16,064) from SNAP [15]. Together the three networks span a range of sizes, densities, and structures, separating the network-specific from the general properties of the influence process.

2.4. Social Network Analysis

To characterize the topology on which the dynamics unfold, we computed a standard battery of social network metrics on the Facebook network using NetworkX 3.6.1 [20]. We measured the degree distribution and its tail behavior (mean, median, maximum, and a maximum-likelihood estimate of the power-law exponent); the global clustering coefficient (transitivity) and the average local clustering coefficient, which together index small-world organization [21]; degree assortativity, which captures whether highly connected individuals link to each other; the number and size of connected components; community structure via the Louvain method [22], summarized by the number of communities and the modularity Q; node centrality in degree, eigenvector, and betweenness (the last estimated by sampling 500 nodes); and the average shortest path length. Each metric bears directly on contagion: degree heterogeneity determines the presence of hubs that accelerate spread, clustering and path length govern how quickly emotion traverses the network, community structure locates the boundaries at which influence concentrates, and centrality identifies the specific individuals through whom emotion is most likely to travel.

 doi:10.20944/preprints202609.1987.v1

2.5. Simulation Procedure

Each simulation proceeded in discrete time steps of length $\Delta t = 0.05$, and all nodes were updated synchronously (in parallel) at each step on the basis of the state of the network at the start of the step. A susceptible individual with k neighbors, m of them influenced, was influenced with probability $\beta \cdot (m/k) \cdot \Delta t$, so influence pressure was proportional to the local density of influenced neighbors rather than their raw count. Influenced individuals returned to the susceptible state with probability $\mu \cdot \Delta t$ (natural recovery) or entered the aware state with probability $\alpha \cdot \Delta t$ (aware recovery). Aware individuals decayed to susceptibility with probability $\delta \cdot \Delta t$ and were re-influenced with probability $\beta(1 - p) \cdot (m/k) \cdot \Delta t$. Simulations were initialized with a 2% seed of influenced individuals in an otherwise susceptible network. We ran 30 independent simulations and report means with 95% confidence intervals; the primary outcome was the influenced density, with the aware density tracked in parallel. All runs produced the same qualitative pattern of a rise, a transient peak, and a stable plateau. The simulation code is available as Supplementary Materials (S1–S5).

The normalized exposure (m/k) is a deliberate modeling choice that keeps the agent-based rule consistent with the homogeneous mean-field of Section 2.2. A count-based rule (rate $\beta \cdot m$) would make each individual's exposure grow with their degree, so that hubs are re-influenced and re-infect at a rate proportional to their connectivity; on a heavy-tailed network this yields an effective reproduction ratio scaling with $\langle k^2 \rangle / \langle k \rangle \cdot \beta / (\mu + \alpha)$, which far exceeds the degree-independent R_0 of the normalized rule. Normalizing by k instead makes the expected infection pressure of a node of any degree equal to $\beta \cdot I$ in a well-mixed regime, recovering the mass-action term $\beta \cdot S \cdot I$ of Eqs. (1)–(3) and the degree-independent $R_0 = \beta / (\mu + \alpha)$. This also carries a psychological reading: an individual's affective state depends on the prevalence of the emotion among their social contacts—the fraction of their friends who are influenced—rather than on the raw number of influenced friends, which would overweight large but diluted contact lists. Section 3.4 contrasts the two rules numerically to make the consequences of this choice explicit.

2.6. Parameter Selection and Justification

We treat the model as a theory-building instrument rather than a forecasting tool [16]. Its purpose is to make a verbal account of group emotion executable and to interrogate the qualitative consequences of the two recovery channels, not to reproduce a specific, dated trajectory. Parameters are therefore justified by their relative ordering and by the dynamical regime they place the system in, rather than by point-calibration against a single dataset; the time unit and absolute rates of a discrete-time model are arbitrary, so only scale-invariant features carry meaning. Accordingly, the numerical outcomes reported in Section 3—peaks, plateaus, and densities—are model outputs under this baseline parameter set, not empirical estimates of the prevalence of real emotional states; they are meant to be read for their qualitative ordering and parameter sensitivity rather than as quantitative forecasts.

The transmission rate β is anchored, in order of magnitude, to the empirical estimates of Hill et al. [8], who fitted a contagion model to the Framingham Heart Study and reported transmission rates of 0.02 (happiness) and 0.04 (discontent) per contact per year, with recovery lifetimes of 10 and 5 years (recovery rates of 0.1 and 0.2 per year). We do not import these absolute values; instead we preserve the two scale-invariant features of their estimates. First, transmission is slower than the combined recovery process yet fast enough to sustain spread once aggregated over a contact network. Second, the effective reproduction number lies above unity in the regimes of interest.

The qualitative results of this paper depend only on the sign of $R_0 - 1$ and on the ordering of the four rates, not on their absolute magnitudes. Our conclusions require four conditions: (i) $R_0 = \beta / (\mu + \alpha) > 1$, so that emotional influence is self-sustaining; (ii) $\beta > \mu$, so transmission outpaces natural recovery; (iii) $\mu > \alpha$, so passive fading is faster than the acquisition of regulation capacity; and (iv) $\delta < \alpha$, so that regulation capacity, once acquired, decays slowly. The default parameters ($\beta = 0.35$, $\mu = 0.10$, $\alpha = 0.08$, $\delta = 0.02$) satisfy all four conditions and give $R_0 \approx 1.94$, a moderately supercritical regime in which influence self-sustains without saturating the population, consistent with the qualitative

 doi:10.20944/preprints202609.1987.v1

observation that collective emotional states persist and recur in real groups; no specific empirical value of R_0 is being claimed or calibrated against. (A recent preprint reports a much larger value for emotional contagion, $R_0 \approx 15.6$ [23]; we cite it only for context and do not rest any argument on it, as it has not undergone peer review.)

To verify that our conclusions do not rest on the precise value of β, we swept β across [0.18, 0.50] (equivalently R_0 across [1.00, 2.78]) on the Facebook network, holding the other parameters fixed, and recorded the peak and steady-state influenced densities (30 runs per value; Table 4). The process is near-threshold and fails to self-sustain at $\beta = 0.18$ ($R_0 = 1.00$), becomes a modest but sustained outbreak at $\beta = 0.26$ ($R_0 = 1.44$), and rises monotonically toward saturation as β increases, so the qualitative outcome is insensitive to the precise value of β over a broad supercritical range. Throughout, the qualitative signature—a rise, a transient peak, and a stable endemic plateau—is unchanged; only the height of the plateau moves. The protection factor $p = 0.5$ is a neutral midpoint; the sensitivity analysis (Section 3.4) confirms that varying p, α, or δ shifts the plateau without altering the qualitative pattern.

The ordering $\beta > \mu > \alpha > \delta$ encodes two substantive assumptions. The first, that acquiring regulation capacity is more effortful than passive recovery ($\mu > \alpha$), follows from the emotion-regulation literature: reappraisal and mindfulness training require deliberate practice, whereas an emotion naturally decays [11–13]. The second, that acquired capacity decays slowly ($\delta < \alpha$), reflects the durability of psychological resources documented in the broaden-and-build framework [13]. Both assumptions are behavioral, not numeric, and are therefore robust to any rescaling of the time unit.

3. Results

3.1. Network Structure

The Facebook friendship network is small-world, heavy-tailed, and strongly modular (Table 2). Its 4039 nodes and 88,234 edges give a mean degree of 43.7, but the degree distribution is strongly right-skewed: the median degree is 25, the maximum is 1045, and the standard deviation (52.4) exceeds the mean, indicating a small number of highly connected individuals who act as hubs of potential influence. The complementary cumulative degree distribution decays approximately as a power law over the intermediate range (log–log slope ≈ 1.4, $R^2 = 0.73$, Figure 1), although the bounded ego-network does not exhibit a clean scale-free regime across all scales [24].

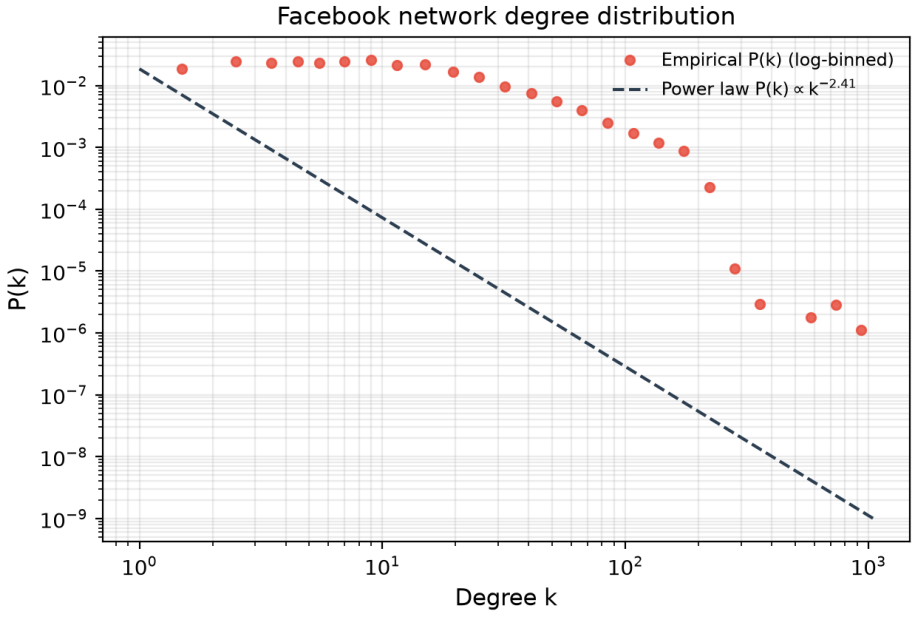

Figure 1. Degree distribution of the Facebook network (log-binned, with a power-law reference).

 doi:10.20944/preprints202609.1987.v1

The network is dense and clustered: the global clustering coefficient is 0.52 and the average local clustering coefficient is 0.61, and the average shortest path length is only 3.69 steps. This combination—short paths with high clustering—is the canonical signature of a small-world network [21], in which emotion can reach any individual through few intermediaries while remaining concentrated within dense local neighborhoods. Degree assortativity is mildly positive (0.064), consistent with social networks in which popular individuals tend to be connected to other popular individuals. The network is fully connected (a single component of 4039 nodes).

The Louvain method partitions the network into 16 communities with modularity Q = 0.83, indicating very strong community structure. Community sizes range from 19 to 548 members, with the five largest communities containing roughly 60% of all individuals (Figure 2). Centrality analysis identifies a small set of individuals who are simultaneously hubs and bridges: node 107 has both the highest degree centrality (0.26) and the highest betweenness centrality (0.49), and a handful of nodes (e.g., 1684, 1912, 3437) rank near the top on multiple measures. Because betweenness centrality counts the fraction of shortest paths passing through a node, these individuals sit at the intersection of many shortest paths and are therefore the natural channels through which emotion crosses community boundaries. In the language of contagion, they are the super-spreaders of the network—relatively few in number, but disproportionately consequential for whether a local affective episode becomes a group-wide one.

Table 2. Social network analysis of the Facebook friendship network.

Metric	Value
Nodes (N)	4039
Edges (E)	88,234
Mean degree	43.7
Median degree	25
Maximum degree	1045
Global clustering (transitivity)	0.52
Average local clustering	0.61
Degree assortativity	0.064
Connected components	1 (fully connected)
Communities (Louvain)	16
Modularity Q	0.83
Average shortest path length	3.69

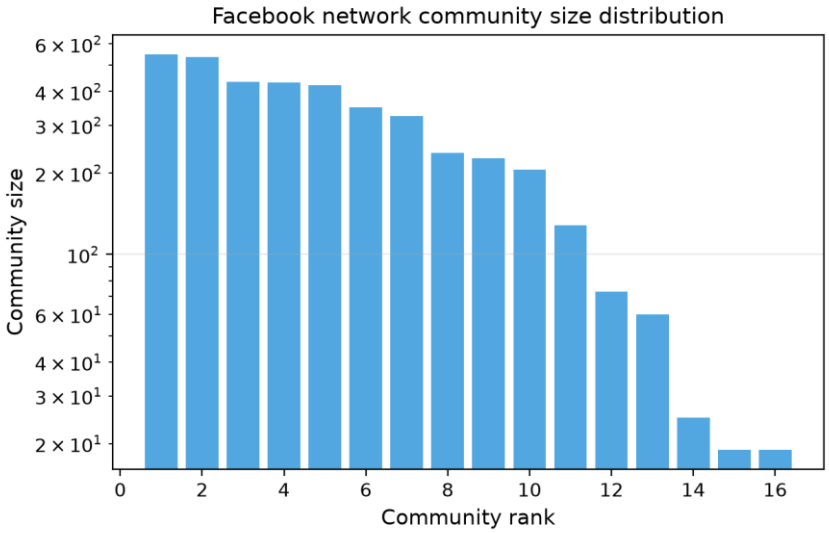

Figure 2. Community size distribution of the Facebook network (logarithmic vertical axis).

 doi:10.20944/preprints202609.1987.v1

3.2. Contagion Dynamics

The model reproduced the characteristic dynamics of emotional contagion on the Facebook friendship network (Figure 3). The influenced proportion rose from a small initial seed, accelerated as influenced individuals in turn influenced their neighbors, reached a transient peak of 32.5% at approximately t = 111, and then settled into a stable plateau at approximately 27.9%. The transient overshoot and subsequent relaxation toward the plateau are consistent with the mean-field prediction that, above threshold ($R_0 > 1$), the system converges to the endemic equilibrium; the plateau is the network counterpart of the endemic state. This rise-and-stabilize pattern is the network-level signature of a self-sustaining influence process.

Three features of these dynamics are meaningful. First, that influence stabilizes rather than dying out or saturating the network reflects the balance between transmission and the two recovery routes. Second, because awareness is acquired from the influenced state and itself decays, the aware proportion rises more slowly and lags behind throughout the episode: it reaches a maximum of 34.2% and stabilizes at 32.3% (Figure 3). During the early accelerating phase, spontaneous awareness formation is not yet sufficient to counteract spread, so proactive regulation is needed to bridge the gap. This lag—between the emotion and the population's capacity to regulate it—is a testable implication distinguishing the model from single-recovery accounts. Third, because the network is organized into dense communities, influence is concentrated within communities early and diffuses across between-group ties later, so community boundaries are natural sites for containment [21,22].

Table 3 summarizes the quantitative outcomes. The fraction ever influenced reaches 98.3%: nearly the entire network experiences the emotion at some point, even though only about half is influenced at any moment—a gap between cumulative and instantaneous exposure that follows from the recovery dynamics. Because the simulation retains the degree heterogeneity, clustering, and community structure of the real network, the simulated plateau need not coincide numerically with the homogeneous-mixing endemic state of Eqs. (5)–(7); the quantitative deviation reflects the network effects that homogeneous mixing ignores [6,7]. The qualitative correspondence is exact, however: both converge above threshold to a stable state with a substantial influenced fraction.

Table 3. Summary statistics of the simulation across the Facebook network and two benchmarks (means over 30 runs).

Network	N	E	Peak influenced	Time to peak (t.u.)	Steady influenced	Steady aware
Facebook	4,039	88,234	0.325	110.7	0.279	0.323
LFR (synthetic)	500	3,769	0.362	104.6	0.266	0.331
email-Eu-core	1,005	16,064	0.354	110.9	0.278	0.312

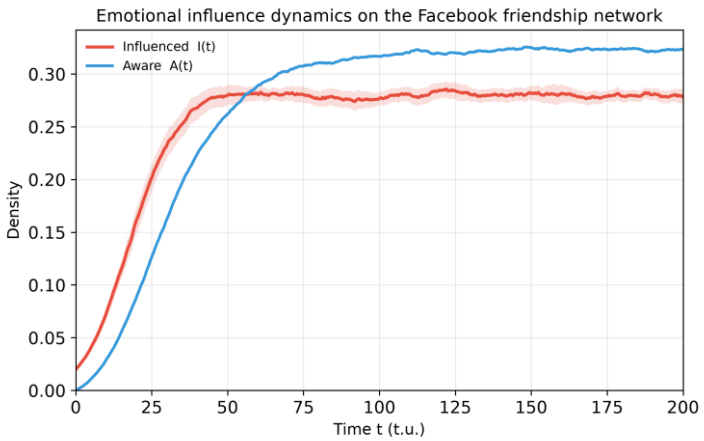

Figure 3. Influenced and aware densities over time on the Facebook friendship network.

 doi:10.20944/preprints202609.1987.v1

3.3. Generalizability Across Networks

A central question for a systems model is whether the emergent behavior is a property of the process or an artifact of the particular topology on which it runs. The same qualitative pattern is reproduced on the two benchmark networks (Figure 4): all three converge to a steady-state influenced density in the narrow band of 27%–28%, each exhibiting the characteristic rise, transient peak, and plateau despite substantial differences in size, density, and structure. Because the qualitative outcome is governed by the sign of $R_0 - 1$, which is positive on all three networks, contact structure shifts the quantitative details of the plateau rather than its existence. The rise-and-stabilize signature therefore reflects a general, structurally robust property of the dual-recovery process—an instance of the kind of macro-level regularity that emerges from micro-level interaction rules regardless of the specific substrate, which is the defining concern of complex-systems modeling.

The one network-specific signature is the likelihood of establishment. The cumulative reach—the fraction of nodes ever influenced—is 100% on the LFR benchmark, 98.3% on Facebook, and 95.0% on email-Eu-core, where occasional realizations fail to cross the 10% threshold altogether. Establishment is thus modulated by the specific topology rather than by size or density alone; once an episode takes hold, however, the rise–peak–plateau signature is unchanged, confirming that the qualitative result is robust to the substrate on which the process runs.

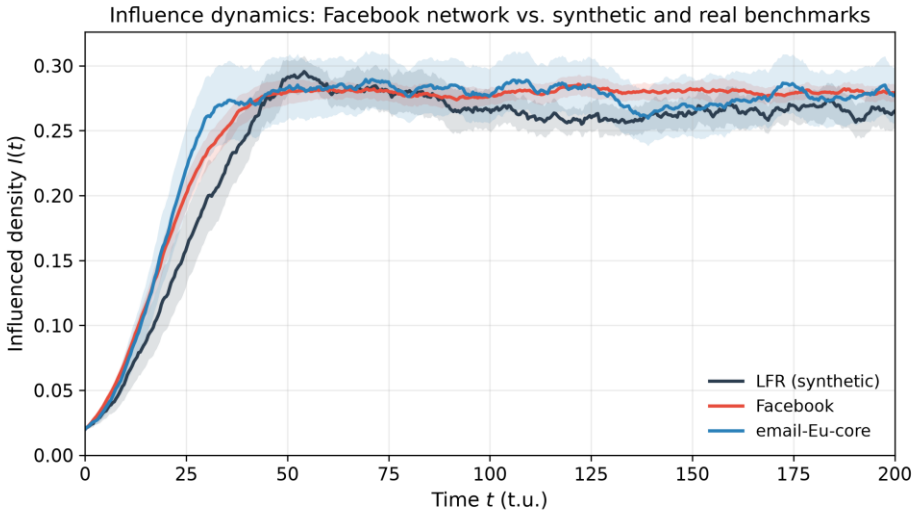

Figure 4. Influenced density (mean with 95% confidence band) over time on the Facebook network and two benchmark networks.

3.4. Sensitivity Analysis

A sensitivity analysis of the steady state is consistent with the analytical derivatives: raising β or δ increases the equilibrium influenced density, while raising μ, α, or p decreases it. That the aware channel moves the equilibrium independently of the natural-recovery channel confirms the model's central claim that the two recovery routes are behaviorally distinct, and it implies that environment-oriented and capacity-oriented interventions have separable, measurable effects on collective emotion. The direction of each effect is interpretable in ordinary terms: more forceful or more durable emotional expression raises the plateau, whereas faster natural fading, faster acquisition of regulation capacity, or stronger protection all lower it.

Table 4 reports the numerical sweep underlying these qualitative statements. The influenced density behaves monotonically: as β increases, R_0 crosses the epidemic threshold and both the peak and the steady-state influenced density rise and then saturate; as α increases (which lowers R_0 by draining the influenced state into the buffered aware state), the plateau declines monotonically. The aware density, by contrast, is non-monotonic in both parameters, exactly as the limit arguments in

 doi:10.20944/preprints202609.1987.v1

Section 2.2 predict. On the Facebook network it rises with β to a maximum at β ≈ 0.35 (R_0 ≈ 1.94) and then declines as re-influence increasingly drains the buffer; and it rises with α to a maximum near α = 0.10 before declining as the shrinking influenced pool starves awareness formation. This interior optimum—rather than a monotone increase—is the empirical signature of the dual-channel interaction: capacity-building produces the largest regulated population at an intermediate, not maximal, intensity.

Table 4. Sensitivity of the peak and steady-state densities to β and α on the Facebook network (means over 30 runs; μ = 0.10, δ = 0.02, p = 0.5).

Parameter	Value	R_0	Peak influenced	Steady influenced	Steady aware
β =	0.18	1.00	0.026	0.008	0.032
β =	0.22	1.22	0.048	0.021	0.078
β =	0.26	1.44	0.134	0.102	0.221
β =	0.30	1.67	0.223	0.180	0.291
β =	0.35	1.94	0.325	0.279	0.323
β =	0.40	2.22	0.400	0.357	0.315
β =	0.45	2.50	0.466	0.426	0.301
β =	0.50	2.78	0.518	0.480	0.281
α =	0.04	2.50	0.517	0.483	0.187
α =	0.06	2.19	0.412	0.375	0.264
α =	0.08	1.94	0.325	0.279	0.323
α =	0.10	1.75	0.234	0.190	0.344
α =	0.12	1.59	0.167	0.117	0.324

Table 5 extends the sweep to the two parameters that govern the aware channel, p and δ. The protection factor p acts monotonically: as p rises from 0.30 to 0.70 the steady-state influenced density falls from 0.372 to 0.173 while the steady-state aware density rises from 0.270 to 0.353, because stronger protection both shields aware individuals from re-influence and, by reducing re-influence, preserves the buffer they constitute. The decay rate δ acts in the opposite direction: as δ rises from 0 to 0.08 the influenced density rises from 0.201 to 0.350 while the aware density falls from 0.472 to 0.195. The δ = 0 endpoint is notable—the aware density is maximal (≈ 0.47) in the absence of decay, matching the Section 2.2 observation that finite decay is what produces the interior optimum. Neither parameter alters the rise–peak–plateau signature; both merely move the plateau, confirming that p and δ tune the quantitative outcome of the aware channel without changing the qualitative dynamics.

Table 5. Sensitivity of the peak and steady-state densities to the protection factor p and the awareness decay rate δ on the Facebook network (means over 30 runs; β = 0.35, μ = 0.10, α = 0.08).

Parameter	Value	Peak influenced	Steady influenced	Steady aware
p =	0.30	0.407	0.372	0.270
p =	0.40	0.365	0.331	0.295
p =	0.50	0.325	0.279	0.323
p =	0.60	0.273	0.225	0.343
p =	0.70	0.239	0.173	0.353
δ =	0.00	0.281	0.201	0.472
δ =	0.01	0.300	0.251	0.375
δ =	0.02	0.325	0.279	0.323
δ =	0.04	0.346	0.310	0.258
δ =	0.08	0.385	0.350	0.195

 doi:10.20944/preprints202609.1987.v1

The exposure-rule choice of Section 2.5 is verified by a direct comparison. Holding the model identical except for the exposure rule, the count-based rule (rate $\beta \cdot m$) saturates the network—a peak of ≈ 0.95 and a steady influenced density of ≈ 0.94—whereas the normalized rule ($\beta \cdot m/k$) produces the moderate plateau of ≈ 0.28 that the empirical literature associates with real collective emotion. The count-based rule concentrates contagion on hubs to the point of near-total infection, so it does not reproduce the partial, self-limiting penetration that motivates a two-channel recovery model in the first place. The normalized rule is therefore the behaviorally defensible specification for emotional influence, in which an individual's exposure depends on the prevalence of the emotion among their contacts rather than on their raw number.

3.5. Structure–Dynamics Coupling: Perturbation Experiments

Section 3.1 characterized the topology; this section tests whether and how that structure shapes the dynamics. We perturbed the Facebook network in two ways and re-ran the model under the baseline parameters. First, we destroyed all non-degree structure—clustering, community organization, and the redundancy of shortest paths—while preserving the exact degree sequence, by repeatedly rewiring edge endpoints at random (a configuration-model randomization that lowers the global clustering coefficient from 0.52 to 0.05). Second, we removed the 1% of nodes with the highest betweenness centrality—the hub-and-bridge individuals that Section 3.1 identified as the channels of cross-community spread—and ran the model on the largest surviving connected component.

Table 6 reports the results. Two findings stand out. First, degree-preserving rewiring raises the plateau modestly (0.279 to 0.304, about 9%) and pushes cumulative reach to 100% (from 98.3%): the strong community structure of the original network does not amplify the epidemic but confines it, so destroying community boundaries lets influence reach the entire population and slightly lifts the plateau. That the plateau moves only modestly despite the wholesale removal of clustering confirms that, under the normalized exposure rule, the endemic prevalence is set primarily by the degree sequence and by $R_0 = \beta/(\mu + \alpha)$—not by clustering. Second, removing the top 1% of hub-and-bridge nodes fragments the network: the largest connected component shrinks from 4039 to 2380 nodes (59%), and the fraction of the original population ever influenced falls from 98.3% to about 56%, even though the plateau within the surviving component is nearly unchanged (0.279 to 0.265). These nodes are thus load-bearing for connectivity and for whether a local episode becomes group-wide—consistent with their high betweenness—while the steady-state prevalence is robust to their removal because it is governed by R_0 rather than by any single node.

Table 6. Effect of structural perturbations on the contagion dynamics (baseline parameters, means over 30 runs). *Ever-influenced fraction within the surviving component; expressed over the original population it is ≈ 0.56.

Network	N	Clustering	Peak	Steady influenced	Steady aware	Ever influenced
Original	4,039	0.52	0.325	0.279	0.323	0.983
Degree-preserving rewired	4,039	0.05	0.351	0.304	0.334	1.000
High-betweenness removed	2,380	0.49	0.308	0.265	0.311	0.950*

4. Discussion

4.1. Theoretical and Methodological Contributions

This paper modeled emotional contagion as a dynamical process with two recovery channels and implemented it on a large real social network. The central result is that the model generates the characteristic dynamics of collective emotion—a rise, a transient peak, and a stable plateau—on a Facebook friendship network, reaching a steady-state influence prevalence of roughly 28% under the baseline parameters. That a model with interpretable parameters produces this signature on a real

 doi:10.20944/preprints202609.1987.v1

topology, without being calibrated to any specific episode, is consistent with the view that the spread and stabilization of collective emotion reflect general properties of the contagion process rather than artifacts of an idealized network; it is a theory-building result rather than an empirical validation against observed emotion time series.

The model makes four contributions to the computational study of social dynamics. First, it adds a dynamic account to a largely static literature on group emotion. Second, it provides an explicit micro-to-macro link, showing how individual-level transition rules generate emergent group-level outcomes—the threshold behavior at $R_0 = 1$ and the endemic plateau. Third, it treats resistance to influence as a dynamic, acquirable state rather than a fixed disposition, offering a mechanism-based target for intervention. Fourth, by characterizing the underlying network, it connects the emergent dynamics to measurable structural features—small-world connectivity, heavy-tailed degrees, and modular community organization.

The model also occupies a distinct position within the computational contagion literature. Where opinion-dynamics models ask how agents assimilate the opinions of similar others and thereby produce consensus, polarization, or fragmentation [25], the present model shifts the focus from opinions to affect and from assimilation to transmission: emotional states are propagated rather than averaged. Relative to single-channel SIS/SIR models [5], the two-channel structure makes recovery two processes rather than one; relative to the awareness-coupled models [9,10], whose awareness is an information state that lowers transmission, the present aware state is a recovery destination—regulation capacity acquired while recovering. This reframing yields two results that a single-channel account cannot produce. First, because the aware channel enters the reproduction ratio symmetrically with natural recovery, $R_0 = \beta/(\mu + \alpha)$, building regulation capacity is a first-order control on whether collective emotion self-sustains, not merely an aid to recovery. Second, the two channels interact so that the steady-state aware density is non-monotonic in both β and α, peaking at an interior optimum: the regulated population is maximized by an intermediate, not maximal, investment in capacity-building. This is also the sense in which the model extends the SIS framework of Hill et al. [8]: where the original SISa model adds a spontaneous infection rate to a two-state SIS process, here we add a third, aware state and split recovery into parallel channels with independent parameters.

The model's predictions are consistent with the empirical record on emotional contagion. The three-degrees-of-separation reach documented in the Framingham data [3] corresponds, in our account, to the short average path length (3.69) of a small-world network: only a handful of intermediaries are needed to carry emotion across the population. The massive-scale transmission observed experimentally online [4] corresponds to the super-spreader structure that our centrality analysis identifies—a small set of hub-and-bridge nodes through which cascades are disproportionately channeled. What empirical studies cannot easily show, and what the model supplies, is the counterfactual structure: how the same process would unfold were one or the other recovery channel strengthened. Recent simulation work on emotional contagion in organizational and online settings [26] converges with this account in treating epidemic-style spreading as a tractable description of collective emotion, while not distinguishing the two recovery routes that are the focus here.

Finally, the model makes the role of the aware state visible in a way a verbal account cannot: the two channels differ in both steady-state effects and timing, yielding a concrete, testable prediction—that the aware density lags the influenced density by a characteristic amount, and that interventions speeding awareness formation narrow this lag before they reduce the plateau. Such a prediction can be evaluated with longitudinal experience-sampling data.

4.2. Implications for Emotion Regulation and Intervention Design

The practical implications below are model-derived hypotheses, not direct policy recommendations: the model is an idealized account and its parameters are not calibrated to a specific

 doi:10.20944/preprints202609.1987.v1

intervention context. The aim is to translate the model's structure into testable, directional expectations for further study rather than prescriptive guidance.

The practical implications follow from the model's structure. Because it separates awareness formation from natural recovery, the model offers a principled basis for allocating intervention resources: environment-changing interventions—speeding the natural decay of an emotional state—can be weighed against capacity-building interventions such as mindfulness- and reappraisal-based training [11,12]. The lag between influence and awareness suggests that proactive training, delivered before an episode peaks, is more valuable than reactive measures applied after collective emotion has stabilized, and the bifurcation at $R_0 = 1$ implies interventions are most cost-effective when applied early. The interior optimum in the aware density adds a non-obvious qualifier, however: the largest regulated population is produced by an intermediate—not maximal—investment, because awareness is generated from the influenced population, so an intervention strong enough to suppress collective emotion also suppresses the state from which regulation capacity is acquired. In organizational settings, this parallels Barsade's ripple effect [2]: leaders can act on the environment or on the person, and the model indicates these are complementary rather than interchangeable.

In a team under deadline pressure, for instance, a leader could reduce the environmental triggers of collective anxiety (raising μ) or invest in training that builds members' reappraisal and mindfulness skills (raising α). The model predicts that the latter route acts more slowly but produces a more durable buffer, because it routes recovery into the aware state, which partially protects against recurrence—a prediction that echoes the broaden-and-build logic of enduring psychological resources [13].

In digital settings, the network findings carry direct implications for the governance of online collective emotion. The heavy-tailed degree distribution and the concentration of betweenness in a few hub-and-bridge nodes imply that a small minority of accounts mediates the flow of emotion across communities; targeted, transparent interventions aimed at these bridges would disproportionately disrupt cross-community cascades. The strong community structure suggests that emotion—including harmful collective states such as panic or mass anxiety—spreads rapidly within communities before leaking across boundaries, which points to community-aware rather than purely global moderation strategies. Because the model predicts that the population's regulation capacity lags the emotion itself, platform designs that foreground emotional self-regulation—through prompts, friction, or wellbeing-oriented features—address the lag directly, whereas designs that merely curb expression treat the symptom rather than the underlying dynamic.

4.3. Limitations and Future Work

Several limitations warrant caution. The model assumes a single emotional valence, a static network, and homogeneous parameters, and its parameters are not yet calibrated against longitudinal data on real emotional contagion; consequently the numerical outcomes reported here (peak ≈ 33%, plateau ≈ 28%) are model-generated quantities under a baseline parameter set rather than empirical estimates of real emotional prevalence. The Facebook ego-network, while realistic, is a convenience sample of overlapping friendship circles rather than a representative population, which limits the generalizability of the exact numerical outcomes. Following Smith and Conrey [16], we regard the model's role as theory building rather than prediction: it sharpens the distinction between passive recovery and active regulation, and generates testable hypotheses—for example, that interventions targeting regulation awareness should outperform those that merely change environmental conditions. Calibrating the five parameters against longitudinal emotion data is an important direction for future work, as are three extensions: node-level heterogeneity, to represent individual differences in susceptibility and regulation capacity; co-evolving networks, which would close the loop between affect and structure that the present model leaves open; and multi-valence dynamics, in which positive and negative emotions interact rather than propagate in isolation.

 doi:10.20944/preprints202609.1987.v1

5. Conclusions

This study modeled emotional contagion as a dynamical process with two recovery channels—natural recovery and aware recovery—and implemented it on a real Facebook friendship network of 4039 individuals. As a theory-building model, it generated the characteristic rise-and-stabilize dynamics of collective emotion, reaching a steady-state influence prevalence of roughly 28% under the baseline parameters, and a social network analysis showed that these dynamics unfold on a small-world, heavy-tailed, strongly modular topology in which a few hub-and-bridge individuals mediate cross-community spread. Two analytical results follow from the dual-channel structure: building regulation capacity lowers the reproduction ratio $R_0 = \beta/(\mu + \alpha)$ directly, making it a first-order control on whether collective emotion self-sustains; and the steady-state regulated population is non-monotonic in both the influence and capacity-building rates, so the most resilient population is produced by an optimal, not maximal, intervention. By separating the two recovery routes, the model distinguishes environment-oriented from capacity-oriented interventions and predicts that the population's regulation capacity systematically lags the emotion itself. These results offer a dynamic, network-grounded account of group affect and a principled basis for targeting emotion-regulation and platform-governance interventions.

Supplementary Materials: The following supporting information can be downloaded at the website of this article: S1: sisa_model.py; S2: config.py; S3: run_real_networks.py; S4: lfr_network.py; S5: compute_facebook_sna.py.

Author Contributions: Conceptualization, H.Z. and M.Z.; methodology, H.Z.; software, H.Z.; validation, H.Z. and Y.W.; formal analysis, H.Z. and Y.W.; investigation, H.Z.; data curation, H.Z.; writing—original draft preparation, H.Z.; writing—review and editing, Y.W. and M.Z.; visualization, H.Z.; supervision, M.Z.; project administration, M.Z. All authors have read and agreed to the published version of the manuscript.

Funding: This research received no external funding.

Institutional Review Board Statement: Not applicable. This study uses anonymized, publicly available network data and does not involve research on human subjects.

Informed Consent Statement: Not applicable. No individual human data were collected.

Data Availability Statement: Publicly available datasets were analyzed in this study. The Facebook friendship network [14] and the email-Eu-core network are available from the Stanford Large Network Dataset Collection (SNAP) [15] at https://snap.stanford.edu/data (accessed on 16 September 2026). The simulation code and analysis scripts are provided as Supplementary Materials (S1–S5). Further inquiries can be directed to the corresponding author.

Conflicts of Interest: The authors declare no conflicts of interest.

Abbreviations

The following abbreviations are used in this manuscript:

Abbreviation	Meaning
SIA	Susceptible–Influenced–Aware
SIS	Susceptible–Infected–Susceptible
SIR	Susceptible–Infected–Removed
SISa	SIS with spontaneous (autonomous) infection
SNAP	Stanford Network Analysis Project
LFR	Lancichinetti–Fortunato–Radicchi
ABM	Agent-Based Model
R_0	Basic reproduction ratio

References

 doi:10.20944/preprints202609.1987.v1

1. Hatfield, E.; Cacioppo, J.T.; Rapson, R.L. Emotional Contagion. Curr. Dir. Psychol. Sci. 1993, 2, 96–100.
2. Barsade, S.G. The Ripple Effect: Emotional Contagion and Its Influence on Group Behavior. Adm. Sci. Q. 2002, 47, 644–675.
3. Fowler, J.H.; Christakis, N.A. Dynamic Spread of Happiness in a Large Social Network: Longitudinal Analysis over 20 Years in the Framingham Heart Study. BMJ 2008, 337, a2338.
4. Kramer, A.D.I.; Guillory, J.E.; Hancock, J.T. Experimental Evidence of Massive-Scale Emotional Contagion through Social Networks. Proc. Natl. Acad. Sci. USA 2014, 111, 8788–8790.
5. Kermack, W.O.; McKendrick, A.G. A Contribution to the Mathematical Theory of Epidemics. Proc. R. Soc. Lond. A 1927, 115, 700–721.
6. Newman, M.E.J. Spread of Epidemic Disease on Networks. Phys. Rev. E 2002, 66, 016128.
7. Pastor-Satorras, R.; Vespignani, A. Epidemic Spreading in Scale-Free Networks. Phys. Rev. Lett. 2001, 86, 3200–3203.
8. Hill, A.L.; Rand, D.G.; Nowak, M.A.; Christakis, N.A. Emotions as Infectious Diseases in a Large Social Network: The SISa Model. Proc. R. Soc. B 2010, 277, 3827–3835.
9. Funk, S.; Salathé, M.; Jansen, V.A.A. Modelling the Influence of Human Behaviour on the Spread of Infectious Diseases: A Review. J. R. Soc. Interface 2010, 7, 1247–1256.
10. Granell, C.; Gómez, S.; Arenas, A. Dynamical Interplay between Awareness and Epidemic Spreading in Multiplex Networks. Phys. Rev. Lett. 2013, 111, 128701.
11. Gross, J.J. Emotion Regulation: Affective, Cognitive, and Social Consequences. Psychophysiology 2002, 39, 281–291.
12. Kabat-Zinn, J. Mindfulness-Based Interventions in Context: Past, Present, and Future. Clin. Psychol. Sci. Pract. 2003, 10, 144–156.
13. Fredrickson, B.L. The Role of Positive Emotions in Positive Psychology: The Broaden-and-Build Theory of Positive Emotions. Am. Psychol. 2001, 56, 218–226.
14. McAuley, J.; Leskovec, J. Learning to Discover Social Circles in Ego Networks. In Advances in Neural Information Processing Systems 25 (NIPS 2012); Curran Associates: Red Hook, NY, USA, 2012; pp. 539–547.
15. Leskovec, J.; Krevl, A. SNAP Datasets: Stanford Large Network Dataset Collection; Stanford University: Stanford, CA, USA, 2014. Available online: https://snap.stanford.edu/data (accessed on 16 September 2026).
16. Smith, E.R.; Conrey, F.R. Agent-Based Modeling: A New Approach for Theory Building in Social Psychology. Personal. Soc. Psychol. Rev. 2007, 11, 87–104.
17. Macy, M.W.; Willer, R. From Factors to Actors: Computational Sociology and Agent-Based Modeling. Annu. Rev. Sociol. 2002, 28, 143–166.
18. Van Kleef, G.A. How Emotions Regulate Social Life: The Emotions as Social Information (EASI) Model. Curr. Dir. Psychol. Sci. 2009, 18, 184–188.
19. Lancichinetti, A.; Fortunato, S.; Radicchi, F. Benchmark Graphs for Testing Community Detection Algorithms. Phys. Rev. E 2008, 78, 046110.
20. Hagberg, A.; Schult, D.; Swart, P. Exploring Network Structure, Dynamics, and Function Using NetworkX. In Proceedings of the 7th Python in Science Conference (SciPy 2008), Pasadena, CA, USA, 19–24 August 2008; pp. 11–15.
21. Watts, D.J.; Strogatz, S.H. Collective Dynamics of "Small-World" Networks. Nature 1998, 393, 440–442.
22. Blondel, V.D.; Guillaume, J.-L.; Lambiotte, R.; Lefebvre, E. Fast Unfolding of Communities in Large Networks. J. Stat. Mech. 2008, 2008, P10008.
23. Sun, X. The Neuroticism Paradox: How Emotional Instability Fuels Collective Feelings. arXiv 2025, arXiv:2510.16046.
24. Clauset, A.; Shalizi, C.R.; Newman, M.E.J. Power-Law Distributions in Empirical Data. SIAM Rev. 2009, 51, 661–703.
25. Castellano, C.; Fortunato, S.; Loreto, V. Statistical Physics of Social Dynamics. Rev. Mod. Phys. 2009, 81, 591–646.
26. Li, S.; Hao, J.; Chai, Y.; Liu, Y.; Feng, T.; Zhu, X. Emotional Contagion Mechanism and Response Strategy Simulation of Corporate Crises from the Perspective of Online Collective Action. Systems 2026, 14, 1.

 doi:10.20944/preprints202609.1987.v1

Academic Editor:

Received: date
Revised: date
Accepted: date
Published: date